Full paper

Transparent and stretchable triboelectric nanogenerator for self-powered tactile sensing

Gengrui Zhao[a,b,1], Yawen Zhang[c,d,1], Nan Shi[e], Zhirong Liu[a,b], Xiaodi Zhang[a,b], Mengqi Wu[a,b], Caofeng Pan[a,b,f], Hongliang Liu[c,*], Linlin Li[a,b,f,**], Zhong Lin Wang[a,b,f,g,**]

[a] Beijing Institute of Nanoenergy and Nanosystems, Chinese Academy of Sciences, Beijing 100083, PR China
[b] School of Nanoscience and Technology, University of Chinese Academy of Sciences, Beijing 100049, PR China
[c] CAS Key Laboratory of Bio-inspired Materials and Interfacial Science, CAS Center for Excellence in Nanoscience, Technical Institute of Physics and Chemistry, Chinese Academy of Sciences, Beijing 100190, PR China
[d] Chongqing University of Science and Technology, Chongqing 400050, PR China
[e] Department of Chemical Engineering, University of California, Santa Barbara, CA, 93106, USA
[f] Center on Nanoenergy Research, School of Physical Science and Technology, Guangxi University, Nanning 530004, PR China
[g] School of Materials Science and Engineering, Georgia Institute of Technology, Atlanta, GA 30332-0245, USA

ARTICLE INFO

ABSTRACT

Wearable electronic devices have attracted numerous attention in tactile sensing, motion detecting, and biomedical signal monitoring. In particular, a wearable and self-powered sensor combining all the merits of sensitivity, transparency, stretchability, and flexibility is highly demanded to adapt human skins. Herein, we report a fully transparent, highly stretchable, and self-powered contact-separation triboelectric nanogenerator (TENG) as a tactile sensor. The TENG consists of a double-network ionogel with the transparency, stretchability, and conductivity as the electrode and one friction layer, and patterned polydimethylsiloxane (PDMS) as another friction layer. The fabricated sensor reaches a maximum sensitivity of $1.76\,\mathrm{V\,N^{-1}}$ when detecting impacting forces in the range of 0.1–1 N. Meanwhile, with good stretchability of the sensor, the triboelectric signals maintain a good linearity with impacting forces at different tensile ratios (0%, 10%, 50%, and 80% strain). These properties enable the sensor to be capable of monitoring a variety of human activities, including finger touching and bending, breathing, and pulse beating. We believe such a transparent, stretchable and self-powered tactile TENG sensor has tremendous application potential in wearable and soft electronics.

1. Introduction

Wearable electronics [1] have begun to spring up in various contexts including transistors [2,3], strain sensors [4,5], energy storage devices [6,7], and displays [8]. For strain sensors, the properties of flexibility, stretchability and transparency are highly desired to adapt human skins. The flexibility and stretchability of most strain sensors are contributed from their active materials whose resistance could change linearly with their dimensions. Several strategies have been developed to realize the stretchability of the active materials. In particular, studies have doped conductive fillers, such as Ag ink [9], carbon nanotube (CNT) [10], metal nanofibers/nanowires [11–13], and carbon black [14,15], into elastomer to form flexible electrodes [16–19]. However, these flexible sensors suffer from poor transparency and stretchability due to the inherent color and inelasticity of conductive fillers. Comparably, transparent elastic conductive hydrogels doping high-concentration ions gain better transparency and stretchability [20], but dehydrated hydrogels become friable and opaque, losing their original transparency and stretchability. Alternatively, some researchers have adopted ionic liquids (ILs) as the active materials, but the liquid mass may give rise to instability issues, as well as signal hysteresis due to the channels encapsulating ILs [21–23]. More recently, Ding *et al.* have reported the synthesis of a high performance ionogel by locking ILs into binary cross-linked polymer networks, yielding improved mechanical strength and conductivity [24].

Despite significant progress in stretchability and transparency, however, wearable sensors still require external power supply to function properly. Triboelectric nanogenerator (TENG) based sensors

---

* Corresponding author.
** Corresponding authors at: Beijing Institute of Nanoenergy and Nanosystems, Chinese Academy of Sciences, Beijing 100083, PR China.
 E-mail addresses: liuhl@mail.ipc.ac.cn (H. Liu), lilinlin@binn.cas.cn (L. Li), zhong.wang@mse.gatech.edu (Z.L. Wang).
 [1] These authors contributed equally to this work.

offer a promising solution for self-powered sensing. Based on the coupling effect of triboelectrification and displacement current [25–27], TENGs efficiently convert ambient mechanical energy into electricity. Advantages of triboelectric devices include flexibility, lightweight implementation, and versatility in material options, which are desirable for wearable electronics [28–30]. Operating modes of TENGs are commonly classified into four types: vertical contact-separation [26,27], single-electrode [31,32], freestanding triboelectric-layer [33], and contacting-sliding [34,35], as well as their derived structures [36–38]. Even though stretchable and transparent TENGs based on hydrogels have been developed, all of them have a single-electrode structure [39–41]. So that triboelectric signals largely depend on the contacting materials, limiting their applications. In addition, the stretchable electrodes of those TENGs are conductive hydrogels formed in aqueous electrolyte solutions, inevitably leading to dehydration of the hydrogels and in turn, deterioration in ionic conductivity and mechanical elasticity [39–41].

Herein, we report a transparent and stretchable tactile sensor that is self-powered by TENG with a contact-separation structure. We incorporate IL-locked ionogel as the electrode and one electrification layer, which is coupled with another layer of patterned PDMS (molded from vinyl record) for triboelectrification. The unique mechanical properties of the ionogels and PDMS provide good stretchability and transparency to the sensor. Moreover, owing to the nonvolatility of ILs, the ionogel maintains a high ionic conductivity to ensure stable performance of the sensor. Combining the self-powered TENG structure with ionogels of high stretchability, transparency, and conductivity, the reported sensor can be integrated in a broad range of applications of wearable electronics.

2. Experimental section

2.1. Fabrication of the transparent self-powered sensor

The preparation of ionogel was conducted following our previous report, and details were shown in Supporting Information [24]. Breifly, liquid polydimethylsiloxane (PDMS, a 10:1 mixture of base and curing agents, Dow Corning Sylgard 184) was spun onto a clean and smooth surface of silicon wafer or vinyl record, and followed by spinning at 1000 rpm min^{-1} for 15 s and 1500 rpm min^{-1} for 60 s. A final 50 μm thick smooth or patterned PDMS film were obtained after curing at 75 °C for 3 h. The TENG was encapsulated between two PDMS layers and the edge was also sealed with PDMS. Between them, there are three layers comprised with an ionogel film on the top, a patterned PDMS film in the middle, and an ionogel film at the bottom. Two Al belts were attached to the two ionogel films for electrical connection, respectively.

2.2. Characterization and measurement

The conductivity of the ionogel was obtained from a four-point probe resistivity measurement system (Probes tech Co. Ltd., China). Impulse force was provided by a linear motor (LinMot E1100) and its magnitude was measured by a commercial force sensor (501F01, YMC Piezotronics INC) mounted on the motion part of the linear motor. The triboelectric output of the self-powered sensor was recorded by a Keithley 6514 electrometer. The mechanical tensile tests were conducted by an ESM301/Mark-10 system. The morphology of the vinyl record and patterned PDMS film were characterized by a field emission scanning electron microscope (Hitachi, SU-8020). The optical transmittance was measured by a Shimadzu UV-3600 spectrometer.

3. Results and discussion

The transparent, stretchable, and TENG-based sensor had a
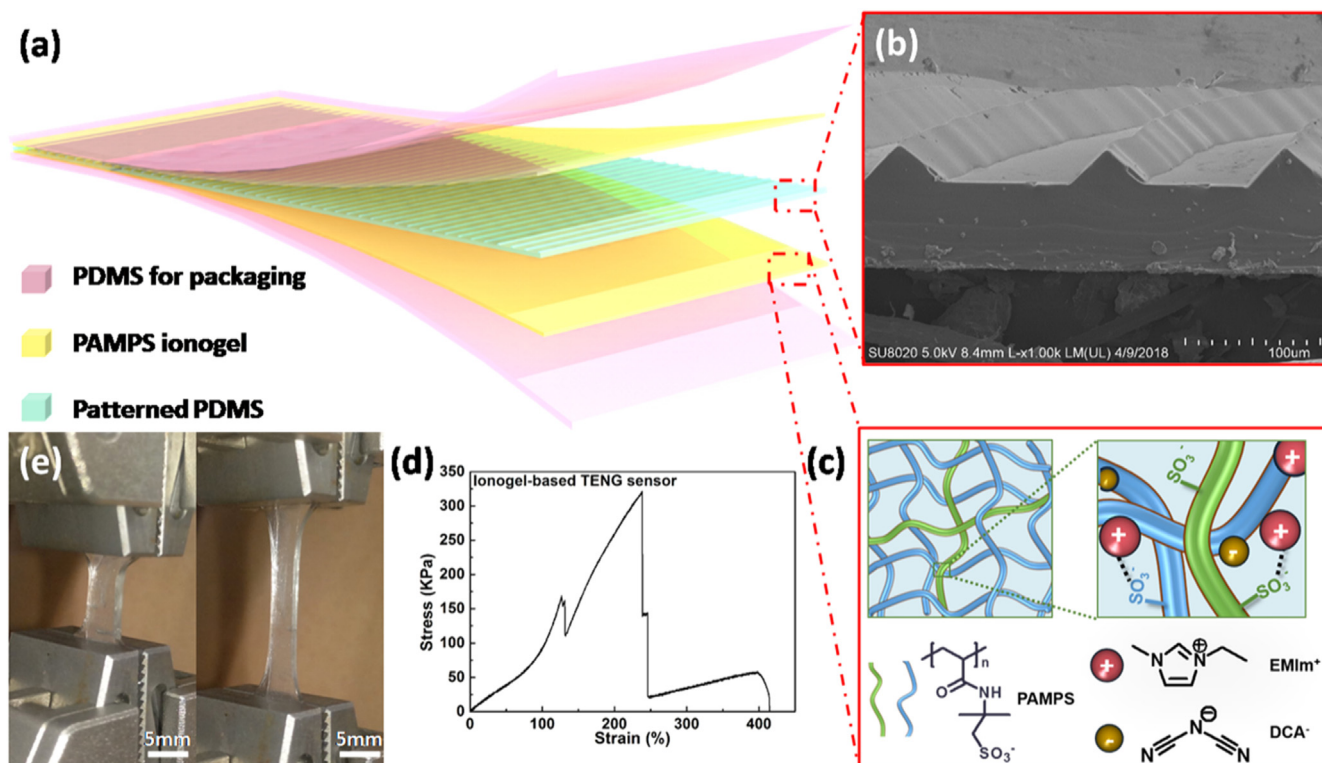
Fig. 1. Structure of the transparent and stretchable TENG-based tactile sensor. a) Layered structure of the sensor. **b)** SEM image of the patterned PDMS film with protruding triangular stripes. **c)** Molecular structure of the ionogel network. **d)** Stress-strain curve of the TENG based sensor. **e)** Photographs of the TENG sensor at original (left) and limiting length before breaking (right).

multilayered structure (Fig. 1a), in which two ionogel films sandwiching a patterned PDMS film were sealed between two smooth PDMS films. PDMS is a common type of materials in biomedical applications and wearable devices because of its transparency, stretchability, biocompatibility and chemical stability [42,43]. Moreover, its negativity in triboelectric series makes it a preferred material of TENG electrification layer [44]. Being similarly triboelectric negative as Teflon, PDMS is more formable, biocompatible and transparent. As an electrification layer of TENG, PDMS film has been intentionally manufactured with topological structures on surface, such as pyramid [26], nanorod arrays [29], and mesopores [30], to increase the friction area. To seek a facile and cost-effective fabrication of PDMS topological structures, we took advantage of the texture structure on a vinyl record's surface to mold a PDMS film with protruding triangular stripes (60 μm wide and 25 μm high) (Fig. 1b, Fig. S1). These protruding triangular stripes on the surface of PDMS film also supported the upper ionogel layer, allowing air gap to be preserved between these two triboelectric layers in the contact-separation TENG.

The electrostatic interaction between the IL [i.e., 1-ethyl-3-methylimidazolium dicyanamide ([EMIm][DCA])] and a charged poly(2-acrylamido-2-methyl-1-propanesulfonic acid) (PAMPS)-based double network allowed us to fabricate a transparent ionogel with both high ionic conductivity (1.9 S m^{-1} at 25 °C) and good mechanical strength [24]. The upper ionogel layer (520 μm thick) functioned as the upper electrode and an electrification layer, while the bottom ionogel film (520 μm thick) acted as the back electrode of the patterned PDMS layer to conduct induced charges. To record the output signal, aluminum (Al) belts were attached to the ionogel films for electrical conduction. The whole TENG device was encapsulated by PDMS films that are 56 μm in thickness, giving a final film structure with a rectangular dimension of 2 × 1.5 cm and thickness less than 1.2 mm.

Attributed to the highly stretchable and transparent PDMS and ionogel, the as-fabricated TENG exhibited excellent transparency and stretchability. From the stress-strain curve of the TENG obtained by uniaxial tensile test, the device had an ultimate stress of 170 kPa at a stretch of 125% strain (Fig. 1d–e). Several cliff falls after the limiting strain were also noticeable in the stress-strain curve, possibly due to

stratified fracture of the whole device induced by relative sliding between the layers and mismatch in their elastic modulus. In fact, the onset of fracture in the ionogel layer at the ultimate strain already suggested the damage and failure of the sensor. Therefore, the following drops in the stress-strain curve only indicted fracture of the other layers and relative motion among those layers. For comparison, the ionogel film had an ultimate stress of 125 kPa at a strain of 121%, while the patterned and smooth PDMS broke down at 122% and 129% strain under 1.7 MPa and 1.5 MPa, respectively (Fig. S2). These values suggested the TENG sensor was first damaged with the fracture of ionogel layer, and then completely failed with the fracture of PDMS films, in consistent with the observation (Fig. S3). In daily life, human epidermal skin is rarely exposed to tension over 100%, allowing the skin-like and ionogel-based sensor to be adapted to stretchable human skin.

The ionogel and smooth PDMS films both achieved a transmittance over 90%, while the transmittance of the molded PDMS film slightly decreased to 85% because of the stripe structure induced refraction (Fig. 2a). Altogether, the 1.2-mm-thick sensor possessed an average transmittance of 83% in the visible light range (400–800 nm wavelength). Despite slightly weakened transmittance, the multilayered structure still allowed vivid image seen through the sensor (Fig. 2a insets).

As a transparent and stretchable electrode, the ionogel film had a favorable conductivity of 1.9 S m^{-1} (Fig. 2b), contributed from the high ionic conductivity of [EMIm][DCA]. More importantly, the good electrical conductivity was not affected by the stress and deformation of the ionogels in practical use. To demonstrate this, the ionogel-based film as a piece of wire was connected with one end of the light-emitting diode (LED) to form a complete circuit with a 5 V direct current voltage source. The conductivity of the ionogel varied between 1.7 S m^{-1} and 2.4 S m^{-1} during stretching and releasing [24]. The brightness of the LED did not change visibly after elongating the ionogel (Fig. 2c-d) or during the reciprocating stretch of the ionogel film (Movie S1). This observation indicated a stable resistance of ionogel films against deformation, as a desired property of electrode materials in TENG.

Supplementary material related to this article can be found online at doi:10.1016/j.nanoen.2019.02.054.
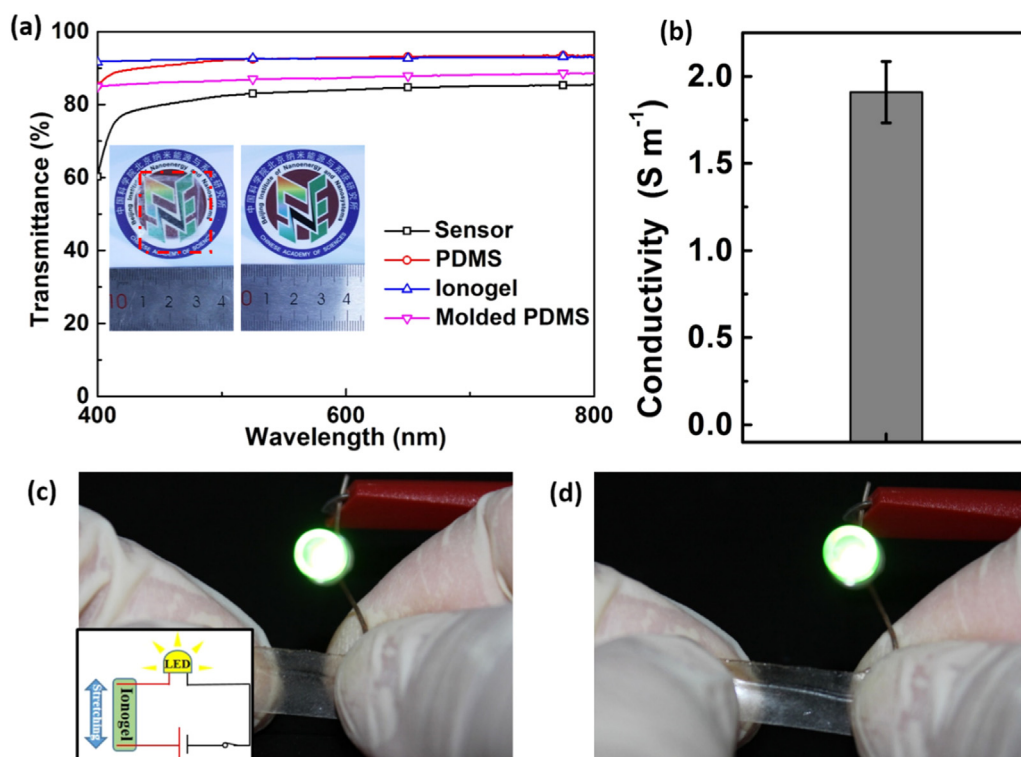
Fig. 2. Transparency and conductivity of the ionogel-based TENG sensor. a) Transmittance of ionogel-based sensor, PDMS film, ionogel film and molded PDMS film in the visible light range. Inset, a sample image seen through the sensor (left, red dashed line indicates the device) and open air (right). **b)** Average conductivity of the unstretched ionogel film. The error bar represents the conductivity variations from ten ionogel samples. The conductivity of the ionogel film, indicated by the brightness of the LED, did not change observably before **c)** and after **d)** stretching. The inset shows the test circuit.
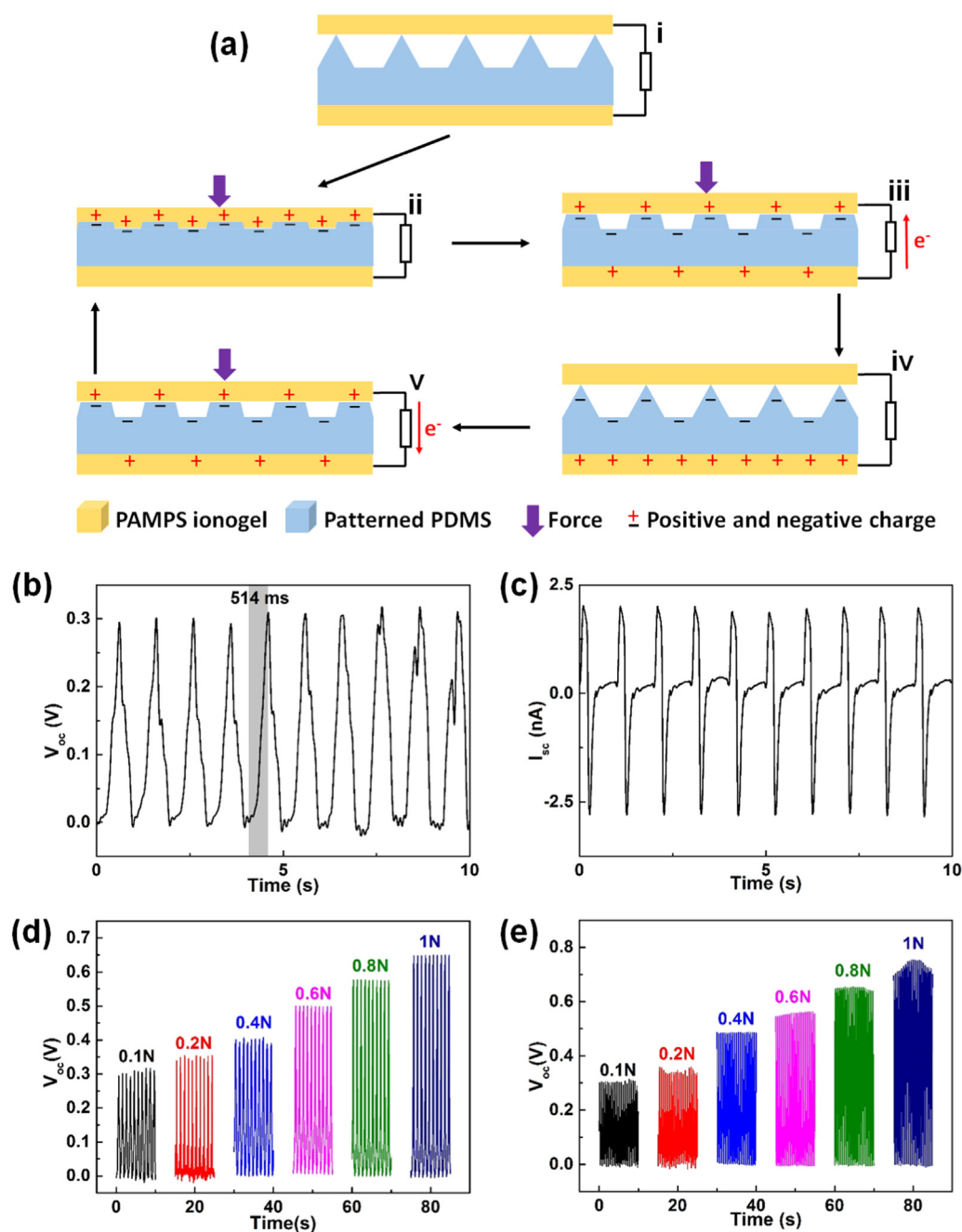
Fig. 3. Working principle and characteristic output of the ionogel-based TENG sensor. a) A complete cycle of the working TENG. **b)** The open-circuit voltage and **c)** short-circuit current of the unstretched sensor induced by 0.1 N impulsive force at 1 Hz. The triboelectric V_{oc} of the unstretched sensor under different magnitudes of impulsive force at **d)** 1 Hz and **e)** 2 Hz.

The working principle of the transparent TENG sensor is based on triboelectrification and electrostatic induction (Fig. 3a). Initially, without pressure on the device, the upper ionogel layer is supported by the tips of the protruding triangular stripes on the patterned PDMS film, and thus separated from the PDMS layer (Fig. 3a, i). When a pressure is imposed, the ionogel layer receives a completely adaptive deformation with the patterned PDMS layer because of their elastic deformation. This is the contacting state (Fig. 3a, ii), in which triboelectrification occurs at the PDMS/ionogel interface. To balance the potential, an equivalent number of positive ions accumulate on the surface of the upper ionogel layer. Later when the pressure is released, the deformation of the two elastomer films would disappear (Fig. 3a, iii). As two surfaces are separating away, positive ions in the bottom ionogel film migrate to balance the static charges on the surface of PDMS.

Meanwhile, a transient flow of charges from the Al connecting tape to the upper ionogel layer generates a current pulse. Finally, when the upper ionogel layer and the PDMS layer recover their initial positions, positive ions on the upper ionogel electrode are completely screened, leaving an equivalent amount of positive ions on the bottom ionogel electrode (Fig. 3a, iv). If pressure is applied on the sensor again, the upper ionogel layer would approach the PDMS layer and the polarity of the electric potential difference would be reversed. In consequence, electrons would flow in the opposite direction (i.e., from the upper ionogel layer to the bottom electrode, Fig. 3a, v). With repeated contact-separation movements between the upper ionogel and patterned PDMS films, an alternative current would be generated.

During detection, a cylinder with a Φ 11.5 mm smooth flat end (the stress surface) was pressed on the top surface of the sensor, giving the

forcing punch a circular contact area (Φ = 11.5 mm). The pressure intensity was about 962.75 Pa with a 0.1 N impulse force. Without being stretched, the TENG sensor outputted a 0.3 V open-circuit voltage (V_{oc}) and 2.3 nA short-circuit triboelectric current (I_{sc}), respectively, under a 0.1 N impulse pressure at the frequency of 1 Hz (Fig. 3b-c).

Strain-resistance elastomer sensor indicated a close correlation between the hysteresis performance in strain-resistance responses and characteristic relaxation of resistance due to elastomer's viscoelasticity [23]. Thanks to the contact-separation structure of the TENG sensor, the deformation of the upper ionogel layer was completely driven by the external force, whereas the electrostatic potentials of the ionogel and PDMS layer largely depended on the distance between the two layers. Therefore, the 514 ms response time corresponded to about one compression stroke from the external force at 1 Hz. Similarly, if the frequency of impulsive force was increased to 2 Hz, the response time of the triboelectricity output dropped to 260 ms, corresponding to one compression stroke in 0.25 s (Fig. S4). In addition, the response time of the sensor kept stable at higher impulsive force. A compression stroke took 543 ms and 552 ms under 0.6 N and 1 N at 1 Hz, as shown in Fig. S5 a-b, respectively.

Fig. 3d shows the triboelectric V_{oc} of the unstretched sensor under different pressure at 1 Hz. The V_{oc} of the TENG was 0.3 V, 0.35 V, 0.4 V, 0.5 V, 0.57 V, and 0.65 V under the pressure of 0.1 N, 0.2 N, 0.4 N, 0.6 N, 0.8 N and 1 N, respectively. Clearly, the triboelectric output of the unstretched sensor increased with larger magnitude of pressure applied at the frequency of 1 Hz. With the impulse frequency maintained at 2 Hz, the triboelectric V_{oc} output of the unstretched sensor increased linearly from 0.3 V to 0.72 V with pressure rising from 0.1 N to 1 N (Fig. 3e). This result suggested that unstretched sensor could also sensitively detect different magnitudes of impacting forces at 2 Hz. Meanwhile, small magnitude of impulsive forces (0.1 N in Fig. S6a and 0.2 N in Fig. S6b) at different frequencies (1–8 Hz) yielded similar triboelectric output (V_{oc}). With the contact area being the same, the similar output of V_{oc} from these cases suggested a fast flow of external electrons to reach equilibrium in the short time of a contact-separation cycle [26,45].

In addition, we characterized the performance of the sensor when subject to different stretching lengths. Under a 10% elongation driven by a small magnitude of impulsive forces (Fig. S6c-d), triboelectric signals of the sensor were sensitive to the frequency of the impulsive forces. Raising the impulsive frequency of 0.1 N pressure from 1 Hz to 8 Hz yielded a 5- fold increase in triboelectric output (from 0.55 V to 2.8 V). Likewise, the triboelectric output increased from 1 V to 1.38 V as the frequency of a 0.2 N impacting force increased from 1 Hz to 8 Hz.
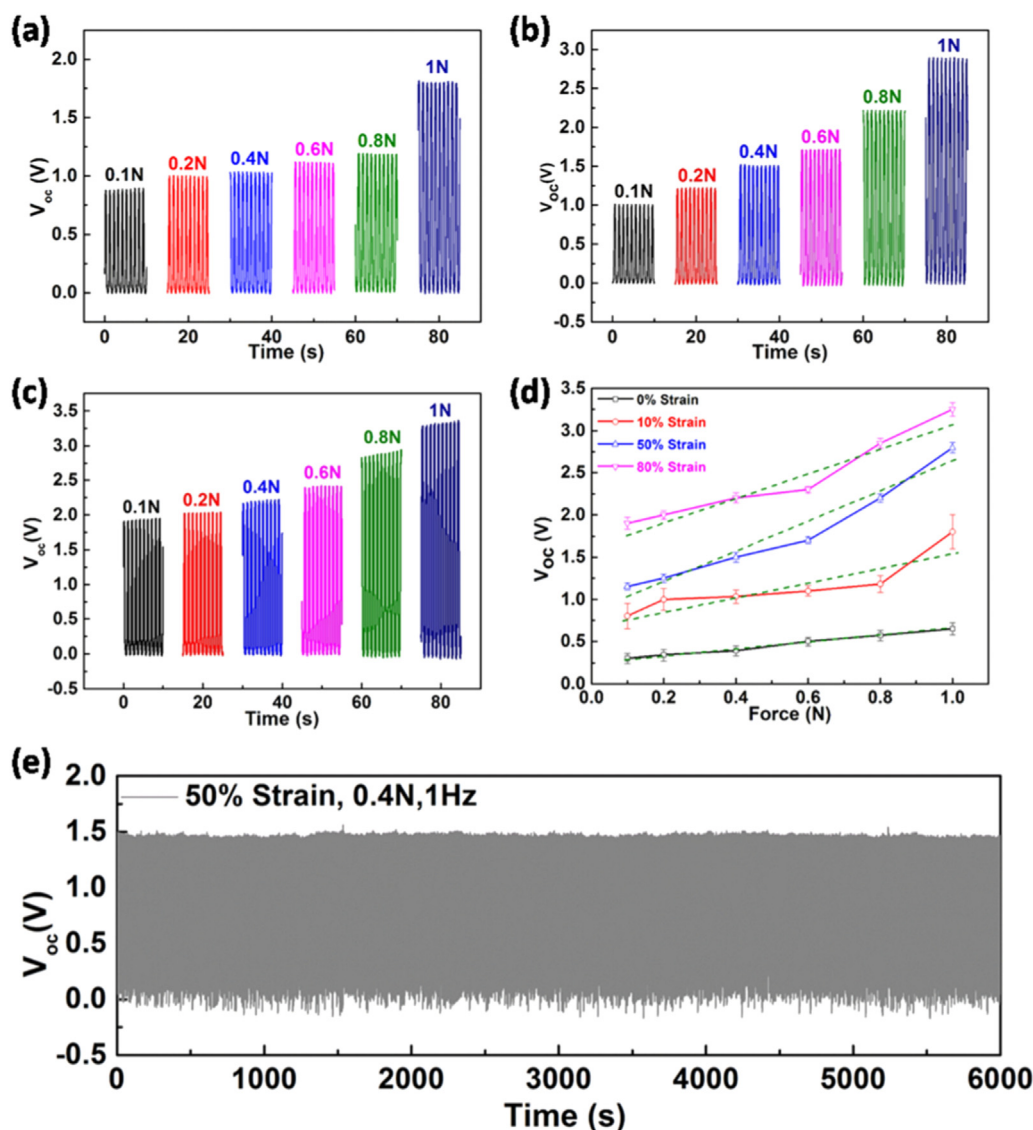
Fig. 4. Triboelectric output (V_{oc}) of the TENG sensor. V_{oc} of the **a)** 10%, **b)** 50% and **c)** 80% strained sensor under different magnitudes of the impulsive force at 1 Hz. **d)** V_{oc} of the sensor at different ratios of tension under different force at 1 Hz. **e)** V_{oc} of the 50% strained sensor under 1 Hz 0.4 N impulsive force over 6000 cycles.

We speculated that, a 10% strain would increase the contacting area, so that the open-circuit voltages were also increased with higher frequency of impacting forces to reach a new equilibrium state. Furthermore, the triboelectric output of a 10% strained TENG increased with stronger impacting force at 1 Hz (Fig. 4a). This correlation was also preserved at a higher impulsive frequency (2 Hz) despite with a weaker trend (Fig. S7).

We further compared the triboelectric output of the ionogel based sensor under a 50% strain driven by forces of different magnitudes and at different impulsive frequencies. Upon the impacting force of 0.1 N, V_{oc} was 1.15 V under 1 Hz and maintained at ~1.3 V when the impulsive frequency increased from 2 Hz to 8 Hz (Fig. S8 a). Under the 0.2 N pressure, however, V_{oc} continuously rose when the frequency of impacting forces increased from 1 Hz to 8 Hz (Fig. S8 b). Regarding the frequency of the impacting forces, we focused on the frequencies below 2 Hz since human skins are rarely subject to vibration frequencies higher than 2 Hz. Within the frequency range, we found a good linear correlation between the triboelectric signal and magnitude of the force. At the 50% strain, V_{oc} increased from 1.2 V to 2.8 V as the 1 Hz

impulsive force increased from 0.1 N to 1 N (Fig. 4b). When the same strain was induced by a 2 Hz impulsive force, V_{oc} was also linearly correlated with the magnitude of the pressure, rising from 1.28 V to 3.3 V when the force increasing from 0.1 N to 1 N (Fig. S9). Under an 80% strain, triboelectric signals of the sensor still manifested changes in the magnitude of impulsive forces at 1 Hz (Figs. 4c) and 2 Hz (Fig. S10). The relationship between the triboelectric signals and the magnitude of impulsive forces at 1 Hz at different stretch ratios are summarized in Fig. 4d. Most importantly, at all the stretching ratios, triboelectric signals clearly increased with increased forces. Finally, because in real applications the strain sensor may subject to impulsive forces over a long period, we also investigated the service life and stability of the self-powered sensor. The 50% strained sensor maintained stable output of triboelectric signals over 6000 cycles driven by a 0.4 N impulsive pressure at 1 Hz (Fig. 4e). It proved that the stretchable sensor could satisfy basic demands of sensing applications.

Having characterized the triboelectrical output of the sensor induced by different pressure, we further quantified the sensitivity of the force sensor using the following equation:
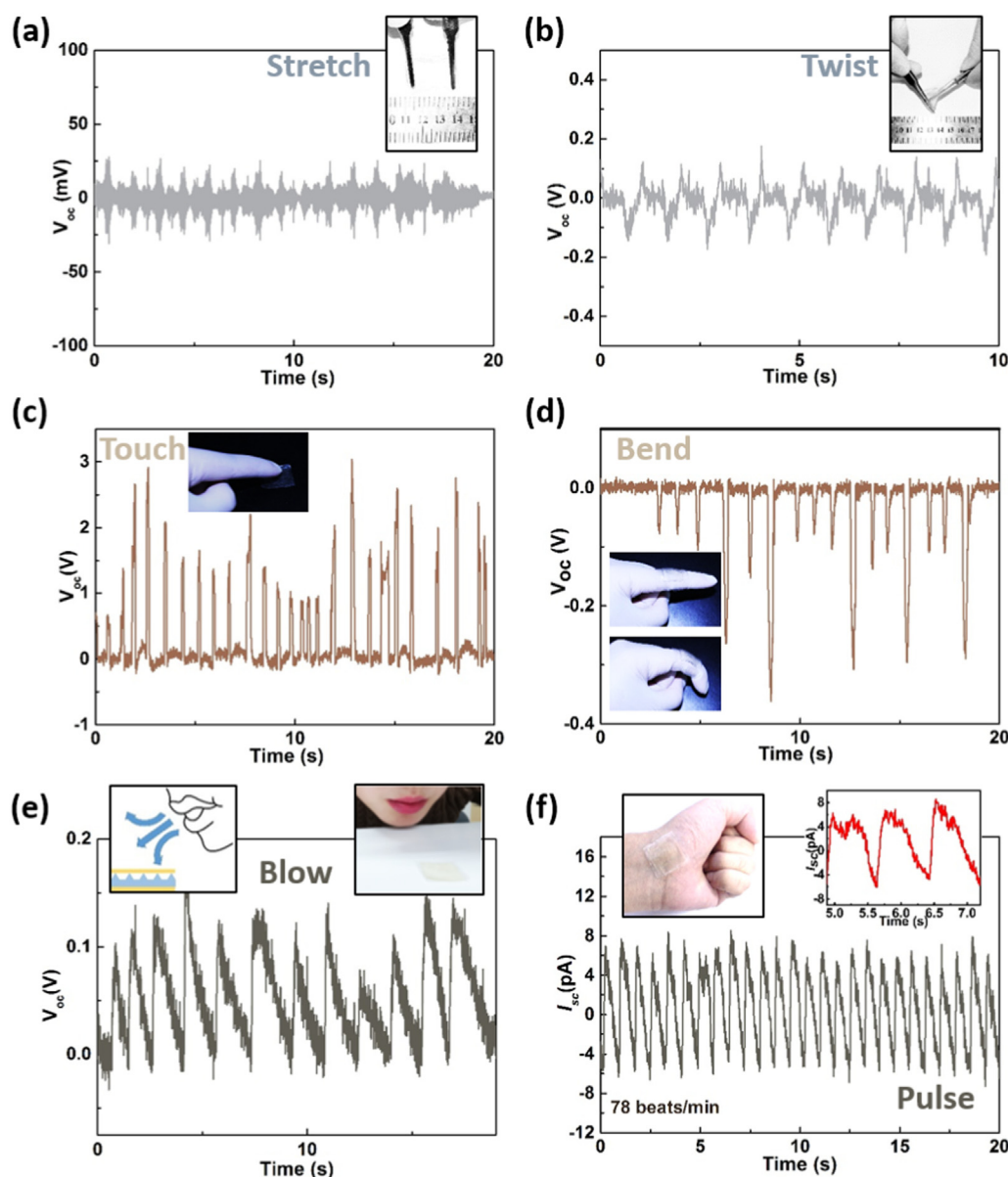
Fig. 5. Self-powered sensor could detect multiple types of motion. The triboelectric signal (V_{oc} or I_{sc}) of the sensor generated by **a)** stretching, **b)** twisting, **c)** touching, **d)** finger bending when the sensor was attached on a finger joint, **e)** airflow blown onto the sensor, and **f)** human pulse beats.

$$GF = \frac{V_{oc}}{F}$$

Where *GF* is gauge factor and V_{oc} is the open-circuit voltage induced by applied pressure *F* on the ionogel sensor. The GF value of the transparent TENG sensor was 0.39, 0.86, 1.76 and 1.46 V N^{-1} at the original sensor length, 10%, 50% and 80% strain, respectively (Table S1). As a stretchable self-powered force sensor, unstretched sensor had the best linearity, followed by the 50% strained one. In addition, the sensitivity increased with the increasing tensile ratio and reached plateau (1.76 V N^{-1}) at the 50% strain. The higher sensitivity and triboelectric signals with increased tensile ratio could be attributed to the increased contact area and shrinking effect of the thickness, simultaneously. The thickness of ionogel and PDMS layer would shrink with the increasing tensile ratio, and thus the displacement between contact surfaces would increase. As a contact-separation TENG sensor, its triboelectric output would increase with increasing displacement.

Being sensitive to pressure and deformation as well as capable of biomedical energy-electricity conversion, the designed TENG device could be applied as a multifunctional wearable sensor to detect multiple types of human motions (Fig. 5). Horizontal stretching of the device yielded weak fluctuation in V_{oc} (~25 mV) (Fig. 5a), which was arised from the slight contact between two triboelectric layers by stretching-releasing reciprocating motion of the sensor. Upon twisted, the sensor outputted V_{oc} with a parallel positive and negative waveform in one cycle with a peak value of 0.1 V (Fig. 5b). In the both cases, even though no normal pressure existed, squeezing and contacting between the patterned PDMS and the ionogel layer occurred during reciprocating twisting.

With high tactile sensitivity, the TENG sensor could detect finger touching (Fig. 5c and Movie S2), where the touching strength was reflected by the magnitude of the triboelectric V_{oc}. Detection of finger bending was realized when the self-powered TENG sensor was attached on the finger joint (Fig. 5d and Movie S3). Furthermore, the sensor could not only detect direct contacting pressure but also the pressure of airflow. When an airflow was blowed near the sensor surface, the strength of induced triboelectric signal reached to the highest 0.18 V (Fig. 5e).

Supplementary material related to this article can be found online at doi:10.1016/j.nanoen.2019.02.054.

The self-powered sensor could also detect pulse beating when attached on wrist. The triboelectric I_{sc} curves of the sensor caused by pulse beating is shown in Fig. 5f. Compared with touching and contacting, throbbing of human skin caused by pulse beating was relatively feeble. The triboelectric I_{sc} of the ionogel sensor reached 8 pA and three I_{sc} peaks took ~2.3 s (Fig. 5f inset). The measured pulse beats of the self-powered sensor were consistent with the volunteer's actual pulse of 78 beats min^{-1} (measured by a commercial OMRON® HEM-7211 sphygmomanometer). The above results demonstrated the excellent performance of the transparent, stretchable, and self-powered TENG sensor for pressure and tactile sensing in wearable electronics.

4. Conclusions

In summary, we have fabricated a transparent and stretchable TENG-based tactile sensor. The TENG structure of the sensor consists of a double network ionogel as its flexible electrode and one triboelectrification layer, and a patterned PDMS layer with dihedral stripes structure as the other triboelectrification layer. The contact-separation motion between the layers of patterned PDMS and highly-conductive ionogel is induced by external impulsive force, which could output stable triboelectric voltage or current for sensing. This sensor has high transparency (83%), good stretchability (121%), and good sensitivity to pressure (0.39–1.46 V·N^{-1}) in the range of 0.1–1 N at different tensile ratios (0%~80%). We demonstrate biomedical applications of this self-powered sensor by detecting touching forces of different magnitudes,

finger bending, human breathing, and pulse beating. With combined transparency, stretchability, and sensitivity, the self-powered skin-like sensor shows great potential in future applications of wearable sensing electronics.

Appendix A. Supporting information

Supplementary data associated with this article can be found in the online version at doi:10.1016/j.nanoen.2019.02.054.

References

[1] J.A. Rogers, Y. Huang, A. Curvy, Stretchy future for electronics, Proc. Natl. Acad. Sci. 106 (2009) 10875–10876.

[2] J.Y. Oh, S. Rondeau-Gagné, Y.-C. Chiu, A. Chortos, F. Lissel, G.-J.N. Wang, B.C. Schroeder, T. Kurosawa, J. Lopez, T. Katsumata, J. Xu, C. Zhu, X. Gu, W.-G. Bae, Y. Kim, L. Jin, J.W. Chung, J.B.H. Tok, Z. Bao, Intrinsically stretchable and healable semiconducting polymer for organic transistors, Nature 539 (2016) 411–415.

[3] G. Schwartz, B.C.K. Tee, J. Mei, A.L. Appleton, D.H. Kim, H. Wang, Z. Bao, Flexible polymer transistors with high pressure sensitivity for application in electronic skin and health monitoring, Nat. Commun. 4 (2013) 1859.

[4] B.C.K. Tee, C. Wang, R. Allen, Z. Bao, An electrically and mechanically self-healing composite with pressure- and flexion-sensitive properties for electronic skin applications, Nat. Nanotechnol. 7 (2012) 825–832.

[5] T. Yamada, Y. Hayamizu, Y. Yamamoto, Y. Yomogida, A. Izadi-Najafabadi, D.N. Futaba, K. Hata, A stretchable carbon nanotube strain sensor for human-motion detection, Nat. Nanotechnol. 6 (2011) 296–301.

[6] S. Xu, Y. Zhang, J. Cho, J. Lee, X. Huang, L. Jia, J.A. Fan, Y. Su, J. Su, H. Zhang, H. Cheng, B. Lu, C. Yu, C. Chuang, T.-i. Kim, T. Song, K. Shigeta, S. Kang, C. Dagdeviren, I. Petrov, P.V. Braun, Y. Huang, U. Paik, J.A. Rogers, Stretchable batteries with self-similar serpentine interconnects and integrated wireless recharging systems, Nat. Commun. 4 (2013) 1543.

[7] Y. Huang, M. Zhong, Y. Huang, M. Zhu, Z. Pei, Z. Wang, Q. Xue, X. Xie, C. Zhi, A self-healable and highly stretchable supercapacitor based on a dual crosslinked polyelectrolyte, Nat. Commun. 6 (2015) 10310.

[8] J. Liang, L. Li, X. Niu, Z. Yu, Q. Pei, Elastomeric polymer light-emitting devices and displays, Nat. Photonics 7 (2013) 817–824.

[9] S.H. Kim, S. Jung, I.S. Yoon, C. Lee, Y. Oh, J.-M. Hong, Ultrastretchable conductor fabricated on skin-like hydrogel–elastomer hybrid substrates for skin electronics, Adv. Mater. 30 (2018) 1800109.

[10] N. Lu, C. Lu, S. Yang, J. Rogers, Highly sensitive skin-mountable strain gauges based entirely on elastomers, Adv. Funct. Mater. 22 (2012) 4044–4050.

[11] S. Gong, D.T.H. Lai, B. Su, K.J. Si, Z. Ma, L.W. Yap, P. Guo, W. Cheng, Highly stretchy black gold E-skin nanopatches as highly sensitive wearable biomedical sensors, Adv. Electron. Mater. 1 (2015) 1400063.

[12] B.W. An, S. Heo, S. Ji, F. Bien, J.-U. Park, Transparent and flexible fingerprint sensor array with multiplexed detection of tactile pressure and skin temperature, Nat. Commun. 9 (2018) 2458.

[13] S. Lee, A. Reuveny, J. Reeder, S. Lee, H. Jin, Q. Liu, T. Yokota, T. Sekitani, T. Isoyama, Y. Abe, Z. Suo, T. Someya, A transparent bending-insensitive pressure sensor, Nat. Nanotechnol. 11 (2016) 472–478.

[14] X. Wu, Y. Han, X. Zhang, Z. Zhou, C. Lu, Large-area compliant, low-cost, and versatile pressure-sensing platform based on microcrack-designed carbon black@ polyurethane sponge for human–machine interfacing, Adv. Funct. Mater. 26 (2016) 6246–6256.

[15] J.-H. Kong, N.-S. Jang, S.-H. Kim, J.-M. Kim, Simple and rapid micropatterning of conductive carbon composites and its application to elastic strain sensors, Carbon 77 (2014) 199–207.

[16] Z. Yang, Y. Pang, X.-l. Han, Y. Yang, J. Ling, M. Jian, Y. Zhang, Y. Yang, T.-L. Ren, Graphene textile strain sensor with negative resistance variation for human motion detection, ACS Nano 12 (2018) 9134–9141.

[17] C. Wang, X. Li, E. Gao, M. Jian, K. Xia, Q. Wang, Z. Xu, T. Ren, Y. Zhang, Carbonized silk fabric for ultrastretchable, highly sensitive, and wearable strain sensors, Adv. Mater. 28 (2016) 6640–6648.

[18] G. Zhao, X. Zhang, X. Cui, S. Wang, Z. Liu, L. Deng, A. Qi, X. Qiao, L. Li, C. Pan, Y. Zhang, L. Li, Piezoelectric polyacrylonitrile nanofiber film-based dual-function self-powered flexible sensor, ACS Appl. Mater. Interfaces 10 (2018) 15855–15863.

[19] Z. Wang, R. Jiang, G. Li, Y. Chen, Z. Tang, Y. Wang, Z. Liu, H. Jiang, C. Zhi, Flexible dual-mode tactile sensor derived from three-dimensional porous carbon architecture, ACS Appl. Mater. Interfaces 9 (2017) 22685–22693.

[20] G. Ge, Y. Zhang, J. Shao, W. Wang, W. Si, W. Huang, X. Dong, Stretchable, transparent, and self-patterned hydrogel-based pressure sensor for human motions

detection, Adv. Funct. Mater. 28 (2018) 1802576.

[21] S.G. Yoon, H.-J. Koo, S.T. Chang, Highly stretchable and transparent microfluidic strain sensors for monitoring human body motions, ACS Appl. Mater. Interfaces 7 (2015) 27562–27570.

[22] S. Russo, T. Ranzani, H. Liu, S. Nefti-Meziani, K. Althoefer, A. Menciassi, Soft and stretchable sensor using biocompatible electrodes and liquid for medical applications, Soft Robot. 2 (2015) 146–154.

[23] D.Y. Choi, M.H. Kim, Y.S. Oh, S.-H. Jung, J.H. Jung, H.J. Sung, H.W. Lee, H.M. Lee, Highly stretchable, hysteresis-free ionic liquid-based strain sensor for precise human motion monitoring, ACS Appl. Mater. Interfaces 9 (2017) 1770–1780.

[24] Y. Ding, J. Zhang, L. Chang, X. Zhang, H. Liu, L. Jiang, Preparation of high-performance ionogels with excellent transparency, good mechanical strength, and high conductivity, Adv. Mater. 29 (2017) 1704253.

[25] F.-R. Fan, Z.-Q. Tian, Z. Lin Wang, Flexible triboelectric generator, Nano Energy 1 (2012) 328–334.

[26] S. Wang, L. Lin, Z.L. Wang, Nanoscale triboelectric-effect-enabled energy conversion for sustainably powering portable electronics, Nano Lett. 12 (2012) 6339–6346.

[27] G. Zhu, C. Pan, W. Guo, C.-Y. Chen, Y. Zhou, R. Yu, Z.L. Wang, Triboelectric-generator-driven pulse electrodeposition for micropatterning, Nano Lett. 12 (2012) 4960–4965.

[28] Z. Lin, J. Chen, X. Li, Z. Zhou, K. Meng, W. Wei, J. Yang, Z.L. Wang, Triboelectric nanogenerator enabled body sensor network for self-powered human heart-rate monitoring, ACS Nano 11 (2017) 8830–8837.

[29] W. Seung, M.K. Gupta, K.Y. Lee, K.-S. Shin, J.-H. Lee, T.Y. Kim, S. Kim, J. Lin, J.H. Kim, S.-W. Kim, Nanopatterned textile-based wearable triboelectric nanogenerator, ACS Nano 9 (2015) 3501–3509.

[30] J. Chen, Y. Huang, N. Zhang, H. Zou, R. Liu, C. Tao, X. Fan, Z.L. Wang, Micro-cable structured textile for simultaneously harvesting solar and mechanical energy, Nat. Energy 1 (2016) 16138.

[31] Y. Yang, Y.S. Zhou, H. Zhang, Y. Liu, S. Lee, Z.L. Wang, A. Single-Electrode Based, Triboelectric nanogenerator as self-powered tracking system, Adv. Mater. 25 (2013) 6594–6601.

[32] Y. Yang, H. Zhang, J. Chen, Q. Jing, Y.S. Zhou, X. Wen, Z.L. Wang, Single-electrode-based sliding triboelectric nanogenerator for self-powered displacement vector sensor system, ACS Nano 7 (2013) 7342–7351.

[33] S. Wang, Y. Xie, S. Niu, L. Lin, Z.L. Wang, Freestanding triboelectric-layer-based nanogenerators for harvesting energy from a moving object or human motion in contact and non-contact modes, Adv. Mater. 26 (2014) 2818–2824.

[34] S. Wang, L. Lin, Y. Xie, Q. Jing, S. Niu, Z.L. Wang, Sliding-triboelectric nanogenerators based on in-plane charge-separation mechanism, Nano Lett. 13 (2013) 2226–2233.

[35] G. Zhu, J. Chen, Y. Liu, P. Bai, Y.S. Zhou, Q. Jing, C. Pan, Z.L. Wang, Linear-grating triboelectric generator based on sliding electrification, Nano Lett. 13 (2013) 2282–2289.

[36] W. Yang, J. Chen, G. Zhu, J. Yang, P. Bai, Y. Su, Q. Jing, X. Cao, Z.L. Wang, Harvesting energy from the natural vibration of human walking, ACS Nano 7 (2013) 11317–11324.

[37] Y. Wu, X. Zhong, X. Wang, Y. Yang, Z.L. Wang, Hybrid energy cell for simultaneously harvesting wind, solar, and chemical energies, Nano Res. 7 (2014) 1631–1639.

[38] Y. Yang, H. Zhang, Z.-H. Lin, Y.S. Zhou, Q. Jing, Y. Su, J. Yang, J. Chen, C. Hu, Z.L. Wang, Human skin based triboelectric nanogenerators for harvesting biomechanical energy and as self-powered active tactile sensor system, ACS Nano 7 (2013) 9213–9222.

[39] X. Pu, M. Liu, X. Chen, J. Sun, C. Du, Y. Zhang, J. Zhai, W. Hu, Z.L. Wang, Ultrastretchable, transparent triboelectric nanogenerator as electronic skin for biomechanical energy harvesting and tactile sensing, Sci. Adv. 3 (2017) e1700015.

[40] T. Liu, M. Liu, S. Dou, J. Sun, Z. Cong, C. Jiang, C. Du, X. Pu, W. Hu, Z.L. Wang, Triboelectric-nanogenerator-based soft energy-harvesting skin enabled by toughly bonded elastomer/hydrogel hybrids, ACS Nano 12 (2018) 2818–2826.

[41] K. Parida, V. Kumar, W. Jiangxin, V. Bhavanasi, R. Bendi, P.S. Lee, Highly transparent, stretchable, and self-healing ionic-skin triboelectric nanogenerators for energy harvesting and touch applications, Adv. Mater. 29 (2017) 1702181.

[42] A. Nag, N. Afsarimanesh, S. Feng, S.C. Mukhopadhyay, Strain induced graphite/Pdms sensors for biomedical applications, Sens. Actuators A Phys. 271 (2018) 257–269.

[43] H.-S. Liu, B.-C. Pan, G.-S. Liou, Highly transparent Agnw/Pdms stretchable electrodes for elastomeric electrochromic devices, Nanoscale 9 (2017) 2633–2639.

[44] A.F. Diaz, R.M. Felix-Navarro, A. Semi-Quantitative Tribo-Electric, Series for polymeric materials: the influence of chemical structure and properties, J. Electrost. 62 (2004) 277–290.

[45] X.-S. Zhang, M.-D. Han, R.-X. Wang, F.-Y. Zhu, Z.-H. Li, W. Wang, H.-X. Zhang, Frequency-multiplication high-output triboelectric nanogenerator for sustainably powering biomedical microsystems, Nano Lett. 13 (2013) 1168–1172.

Dr. Gengrui Zhao received his Ph.D. degree from the University of Chinese Academy of Sciences, China in 2018 from Prof. Linlin Li's group. He received his Master degree from School of Petrochemical Technology at Lanzhou University of Technology in 2015. His research interests include micro-nanomaterials and their applications in flexible electronics and wearable sensors.

Yawen Zhang is currently a master degree candidate under the supervision of Professor Hongliang Liu at Technical Institute of Physics and Chemistry, China. He received his bachelor degree from Chongqing University of Science and Technology. His research interests is the fabrication of high mechanical ionogel and their applications in flexible sensor.

Dr. Nan Shi was a Postdoctoral Research Associate in the Chemical Engineering Department at University of California, Santa Barbara. His research interests include colloidal and interfacial phenomena induced by chemical gradients, microfluidics, and transport phenomena. He received Ph.D. degree in Chemical Engineering from Texas A&M University, United States. His current affiliation is the Reservoir Engineering Technology Division (RETD) at the Exploration and Petroleum Engineering Center - Advanced Research Center (EXPEC ARC), Saudi Aramco, Saudi Arabia.

Zhirong Liu received her undergraduate degree from China University of Geosciences in 2016. Currently she is pursuing her Ph.D. under the supervision of Prof. LinLin Li at Beijing Institute of Nanoenergy and Nanosystem, Chinese Academy of Science. Her research is mainly focused on functional nanomaterials/nanodevices for biomedical applications.

Xiaodi Zhang is currently studying for the doctor degree in Beijing Institute of Nanoenergy and Nanosystems, Chinese Academy of Sciences. Her main research interests focus on application of piezoelectric biomaterials in tissue engineering.

Mengqi Wu received her undergraduate degree from Henan Polytechnic University in 2017. Currently she is a graduate student of Prof. LinLin Li at Beijing Institute of Nanoenergy and Nanosystem, Chinese Academy of Science. Her research is mainly focused on nanomaterials in disease therapy.

Dr. Linlin Li is a professor at Beijing Institute of Nanoenergy and Nanosystems, CAS. She received her Ph.D degree in Physical Chemistry from Technical Institute of Physics and Chemistry, Chinese Academy of Sciences in 2008. Her research interests include biomedical application of nanomaterials and nanodevices in cancer theranostics, biosensoring, and tissue regeneration. Details can be found at http://www.escience.cn/people/linlinnano.

Dr. Caofeng Pan received his B.S. degree (2005) and his Ph.D. (2010) in Materials Science and Engineering from Tsinghua University, China. He then joined the Georgia Institute of Technology as a postdoctoral fellow. He is currently a professor and a group leader at Beijing Institute of Nanoenergy and Nanosystems, Chinese Academy of Sciences since 2013. His main research interests focus on the fields of piezotronics/piezo-phototronics for fabricating new electronic and optoelectronic devices, nano-power source (such as nanofuel cell, nano biofuel cell and nano-generator), hybrid nanogenerators, and self-powered nanosystems. Details can be found at http://piezotronics.binncas.cn.

Zhong Lin Wang received his Ph.D. from Arizona State University in physics. He now is the Hightower Chair in Materials Science and Engineering, Regents' Professor, Engineering Distinguished Professor and Director, Center for Nanostructure Characterization, at Georgia Tech. Dr. Wang has made original and innovative contributions to the synthesis, discovery, characterization and understanding of fundamental physical properties of oxide nanobelts and nanowires, as well as applications of nanowires in energy sciences, electronics, optoelectronics and biological science. His discovery and breakthroughs in developing nanogenerators established the principle and technological road map for harvesting mechanical energy from environment and biological systems for powering personal electronics. His research on self-powered nanosystems has inspired the worldwide effort in academia and industry for studying energy for micro-nano-systems, which is now a distinct disciplinary in energy research and future sensor networks. He coined and pioneered the field of piezotronics and piezophototronics by introducing piezoelectric potential gated charge transport process in fabricating new electronic and optoelectronic devices. Details can be found at: http://www.nanoscience.gatech.edu.

Dr. Hongliang Liu is currently an associated professor at the Technical Institute of Physics and Chemistry, Chinese Academy of Sciences. He received his B.Sc. degree in organic chemistry (2005), and Ph. D. degree in polymer chemistry and physics (2010) from Lanzhou University. He then worked as a postdoctoral fellow (2011–2014) in Prof. Lei Jiang's group at the Institute of Chemistry, Chinese Academy of Sciences. His current scientific interest is focused on fabrication of multi-scale surfaces with controllable superwettability, and their applications on advanced functional materials.